INVESTIGATION OF THE EFFECT OF HEATING RAMPING RATE ON Cu(In, Ga)Te$_2$ THIN FILMS

Serkan ERKAN[1,*] ⓘ**D**, **Yavuz ATASOY**[2] ⓘ**D**, **Ali ÇİRİŞ**[3] ⓘ**D**, **Emin BACAKSIZ**[4] ⓘ**D**

1,2,3 Niğde Ömer Halisdemir University, Nanotechnology Application and Research Center, 51240 Niğde
2. Niğde Ömer Halisdemir University, Niğde Zübeyde Hanım Health Services Vocational High School, 51240 Niğde
4. Karadeniz Teknik University, Faculty of Science, Department of Physics, 61080 Trabzon

ABSTRACT

Cu(In,Ga)Te$_2$ (CIGT) thin films were grown using a two-stage method. In the first stage, (Cu, In, Ga) precursor layers were grown on Mo coated flexible stainless steel substrates using the electro-deposition method. NaF and Te layers were grown on metallic precursor layers using electron beam evaporation method. In the second stage, the foil/Mo/(Cu, In, Ga)/NaF/Te stacks were reacted at 600°C for 5 minutes by rapid thermal processing. The temperature ramping rates in this procedure were 0.5°C/sec, 1°C/sec, 5°C/sec and 10°C/sec. In order to investigate the effect of temperature ramping rate on the structural properties of CIGT thin films, XRD, Raman, SEM and EDS measurements were performed. Regardless of the ramping rates, it was determined that all samples crystallized in chalcopyrite structure. According to the Raman spectra, as the ramping rate increased, position of the A$_1$ mode completely changed and shifted from 127 cm^{-1} to 135 cm^{-1} due to bond-stretching forces between the nearest-neighbor atoms. It was concluded that CIGT thin film reacted with a ramping rate of 5°C/sec had superior properties compared to other samples.

Keywords: Cu(In,Ga)Te$_2$, Heating ramping rate, Two-stage process, Electro-deposition

1. INTRODUCTION

Ternary and quaternary absorber layers such as Cu(In)(S,Se,Te)$_2$ [1-4], Cu(Ga)(S,Se,Te)$_2$ [5-7] and Cu(In,Ga)(S,Se,Te)$_2$ [8-11] which are consisting of elements of the I-III-VI$_2$ group have an important potential in photovoltaic (PV) applications. In addition, the small area Cu(In,Ga)(S,Se)$_2$ (CIGSSe) cells were reported to have a photo-conversion efficiencies of over 22% [12, 13]. These compounds that crystallize in chalcopyrite structure have high optical absorption coefficient ($>10^4$ cm^{-1}) and direct transition band structure. In addition to these features, the band gap of this absorber material is adjusted by altering the compositions of the constituent elements. For example, the band gap of CIGSSe varies between 1.00 eV to 1.72 eV depending on the amount of Ga and/or S in the compound [14]. Similarly, the band gap of the Cu(In,Ga)Te$_2$ (CIGT) compound varies in the range of 0.96 eV (CuInTe$_2$) -1.35 eV (CuGaTe$_2$) [15].

There have been many studies focusing on changing the amount of Ga in place of In in the CIGSSe thin films. In one of these studies, Cu(In,Ga)Se$_2$ (CIGS) thin films were produced using a two-step method with the goal of varying the atomic ratios of [(Ga)]/[(Ga)+(In)]. In the grown samples, it was seen that Ga was inhomogeneously distributed through thickness of the film, accumulated near to Mo-back contact and had Se-rich of the film surface. This distribution of the Ga causes the formation of compositional non-uniformity resulting SLG/Mo/CGS/CIS type structure which reduces solar cell efficiency. However, it was found that the diffusion of Ga towards the surface of the film became easier with the increase of the annealing temperature (≥575°C) [16]. To investigate the effect of Cu content on the structural properties such as phase evaluation and crystallinity of the CIGS thin films, Witte et al. produced CIGS thin films with various amount of Cu by an in-line co-evaporation process. According to the Raman spectra of the samples, it was observed that A$_1$ modes shifted to low values with increasing Cu content. Furthermore, the full width at half maximum (FWHM) values of the A$_1$ mode decreases with increasing Cu content, due to the better crystallinity and reduced disorder in the films [17]. Rudmann et al. prepared CIGS layers using DC sputtering on Mo coated soda-lime glass substrates (SLG) to investigate the impact of Na diffusion on the properties of CIGS. According to scanning electron microscope (SEM) images, they observed a reduction in grain size of the films in the presence of Na during growth [18]. However, the studies on telluride quaternary compounds are quite limited. Gremenok et al. produced the

INVESTIGATION OF THE EFFECT OF HEATING RAMP RATE ON CU(IN, GA)TE$_2$ THIN FILMS

$CuGa_xIn_{1-x}Te_2$ thin films by changing the amount of Ga. As a result of the X-ray diffraction (XRD) analysis, it was seen that thin films crystallized in chalcopyrite structure, with a preferential orientation along (112). They revealed that the lattice parameters and band gaps of the samples changed linearly with the amount of Ga [19]. Sanad et al. produced CIGT thin films with micron and sub-micron thicknesses using a simple co-precipitation method to get high-performance photogene materials in PEC solar cell devices. They observed that crystallographic and morphological properties can be easily controlled by changing the In^{3+}/Ga^{3+} molar ratio [20]. Gaburicci et al. reported on polycrystalline bulk $CuIn_{1-x}Ga_xTe$ samples with the different atomic ratios of 'x' (x= 0 - 1) by using rapid cooling technique. XRD measurements have shown that all samples crystallized in chalcopyrite structure, however In_2Te_3 secondary phase formed. They reported that the rapid cooling technique is very suitable for indium-rich compounds, but not for gallium-rich compounds [21]. In another study, Rincon et al. examined the relationship between Urbach energy and temperature for $CuInTe_2$ compound. The vibration modes of chalcopyrite structures of different compounds such as $CuGa_3Te_5$, $CuIn_3Te_5$, $CuIn_5Te_8$ were also examined by the same research group [22-26].

In this study, CIGT thin films were grown using a two-step method. In the first stage, (Cu, In, Ga) metallic precursors were grown by electro-deposition method followed by Te and NaF layers were evaporated over the metallic precursors using electron beam system. In the second stage, the resultant layered-structures were reacted with different ramping rates at the targeted temperature by rapid thermal processing (RTP). The effect of different ramping rates on the structural properties of CIGT samples are examined in detail.

2. MATERIAL AND METHOD

CIGT samples were produced using a two-stage method. In the first stage of the method, Cu-In-Ga metallic layers were deposited on the Mo coated 304 stainless steel foil by using an electro-deposition system. Detailed information about the electro-deposition of Cu, In, Ga layers are found in previous studies [15, 27]. The thickness of the Cu, In and Ga films grown by electro-deposition method were determined individually by counting the loads passed on the stainless-steel substrate [23]. The thickness of stainless steel foil and Mo back contact layer is 50 μm and 1.5 μm, respectively. Theoretical and experimental studies on CIG(S,Se) thin films produced with different atomic ratios show that the best solar cell efficiency value is obtained from Cu-poor and low Ga-doped absorption layers [13]. Therefore, the stoichiometric ratio determined for metallic layers is about 0.3 for [Ga]/([Ga]+[In]) and 0.7-0.9 for [Cu]/[In]+[Ga]). The nominal thickness of Cu-In-Ga layers corresponding to these ratios were determined as 160, 270 and 90nm, respectively. NaF (3N) [25] and Te (5N) layers were evaporated over the Cu-In-Ga layers using with electron beam system. In the second stage, (Cu, In, Ga)/NaF/Te stacks were thermally annealed in an RTP furnace. The ramping rates of 0.5, 1, 5 and 10 °C/sec were employed for annealing process. Annealing process was carried out in Ar atmosphere, at the target temperature of 600°C for 5 minutes. Heat treatment of the samples was performed in RTP furnace.

XRD measurements of the samples were performed in the range of 2θ = 20°–70° using the Rigaku SmartLab unit (λ = 1,5405 Å) with CuKα source at room temperature. Raman spectra were obtained with the Renishaw-INVI Reflex Confocal Raman System using a 532 nm laser excitation source at room temperature. SEM images were taken with JEOL JSM 6610 scanning electron microscope. The compositions of the growth films were determined using Oxford Instruments Inca X-act EDS Analysis Unit.

3. RESULTS AND DISCUSSION

3.1. X-Ray Diffraction (XRD) Spectra

XRD spectra of CIGT thin films reacted with different ramping rates are shown in Figure 1. In addition, 2θ diffraction angles and d-spacing values of the main peak are given in Table 1. When the figure and table were examined, it was seen that all samples crystallized in chalcopyrite structure irrespective of the ramping rates. All characteristic peaks of the chalcopyrite structure (112), (220/024) and (312/116) were observed in diffraction patterns of all samples (JCPDS Card No: 00-049-1326) [28]. Besides, it was determined that peaks appeared at 2θ = 40.5° and 58.5° are associated with the Mo back contact (JCPDS Card No: 00-042-1120). As can be seen in Table 1, the 'd' values corresponding to the peak positions (112) are in the range of 3.53-3.55 Å for all samples. The lattice parameter 'a' corresponding to these d-values were also calculated using Equation 1 [29],

S. Erkan, Y. Atasoy, A. Çiriş, E. Bacaksız

$$a = \left(\frac{d}{2}\right)\sqrt{4\left(h^2 + k^2\right) + l^2} \tag{1}$$

where (h, k, l) are Miller indices. For tetragonal structures, these indices are h =1, k = 1 and l = 2. In addition, the crystallite sizes of the samples were calculated with the Scherer formula in Equation 2 [30, 31].

$$D_{(h,k,l)} = \frac{0.9\lambda}{\beta\cos\theta} \tag{2}$$

where λ is the X-ray wavelength, β is the FWHM of (112) peak and θ is the diffraction angle. The calculated values by using Equation 2 were given in Table 1. It was observed that the samples reacted with 0.5, 1 and 10 °C/sec had high FWHM values, indicates the samples may consist of compounds with different Ga-gradients throughout the thin film. In a recent study, the Ga distribution of CIGT films produced using a two-stage method was examined by angle dependent-XRD analysis. It was confirmed that the films represent a series of Ga compositions throughout the layer, resulting in higher Ga content near the back contact [25, 32].

According to the XRD spectra of our samples, it was observed that the (112) peak intensity increased with the increase ramping rate, reached maximum value for the sample reacted with 5°C/sec, then decreased again with the increment of the ramping rate. In addition to this, sample reacted with 5°C/sec has the lowest FWHM value (0.18°) and a sharper peak. Within this context, the best crystallization was shown in the sample reacted with ramping rate of 5 °C/sec.

It was concluded that no secondary phases were observed in all samples regardless of the ramping rate. The formation of a single phase structure indicates that the dwell time used in the process is sufficient [25]. On the other hand, in the last column of the Table 1, the ratio of the Mo to CIGT main peak intensities (I_{Mo}/I_{CIGT}) is given. Although Mo peak intensity is the lowest for 10 °C/sec, the ratio of I_{Mo}/I_{CIGT} is the highest value. For the samples reacted with 0.5, 1 and 5°C/sec, the ratio of I_{Mo}/I_{CIGT} varied in the range of 0.38-0.40.
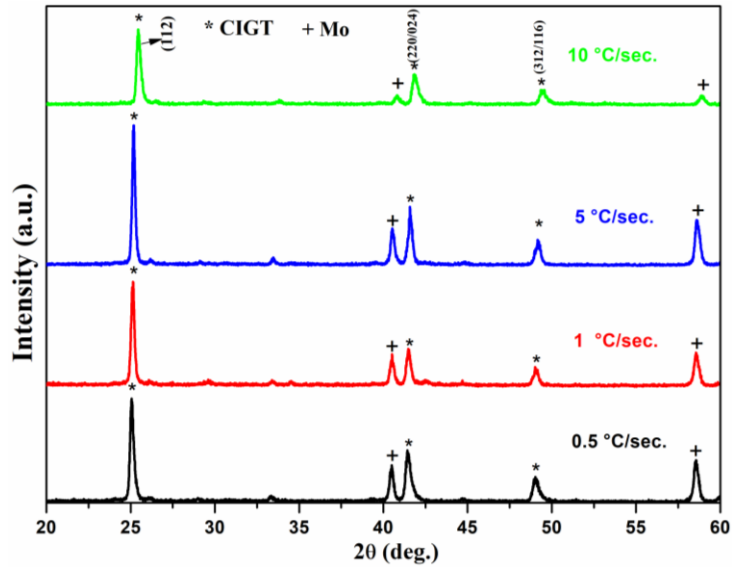

Figure 1 XRD spectra of CIGT thin films reacted with different ramping rates

Table 1 Some structural parameters calculated based on (112) main peak in the XRD spectra

Ramping rate (°C/sec)	2θ (°)	d (Å)	a (Å)	β_{FWHM} (°)	Crystal size (nm)	$I_{Mo}/I_{(112)}$
0.5	25.05	3.55	6.15	0.24	34.04	0.38
1	25.07	3.54	6.14	0.23	35.87	0.40
5	25.11	3.54	6.13	0.18	43.16	0.39
10	25.20	3.53	6.12	0.22	36.39	0.46

INVESTIGATION OF THE EFFECT OF HEATING RAMP RATE ON CU(IN, GA)TE₂ THIN FILMS

3.2. Raman Spectra

Raman spectra of CIGT films reacted with the ramping rates are given in Figure 2. The Raman shifts and corresponding of the Raman modes of our samples and their related reference values are given in Table 2. As can be seen in Figure 2, Raman peaks were observed at 106, 117, 128 and 170 cm^{-1} for the lowest ramping rate (0.5 °C/sec). These peaks are attributed to B_2^2, B_1^2, A_1 and E^5 or B_2^3 vibrational modes, respectively [25]. The dominant A_1 mode located at 128 cm^{-1} depends on the planar motion of the cation and anion (tellurium) atoms. Also, large-shaped phonon frequencies around 200 cm^{-1} may be attributed to the combination of E and B_2 modes [26]. These peaks seen in the Raman spectra are consistent with the reported values in previous studies [23-26].

In Raman spectra, it was seen that there were small shifts in the peak positions with the ramping rate in the range of 0.5-5°C/sec. However, the Raman spectrum of 10°C/sec was completely changed. This change can be clearly seen in the inset of Figure 2, which demonstrates the expanded form of A_1 modes in the spectra. Besides, when the ramping rate is increased from 0.5 to 1°C/sec, there is a slight shift in the main peak and a new shoulder appeared next to the main peak. The resulting phase separation indicates different Ga compositions through the film, as stated in the XRD section. It shows that this phase has changed completely from CIGT to CGT with shifting of the main peak from 127 cm^{-1} to 135 cm^{-} for the sample reacted with 10°C/sec. This situation may result from the changing of the surface morphology, the deviation of film stoichiometry (especially Ga amount) or bond stretching forces between the nearest-neighbor atoms [33, 34].
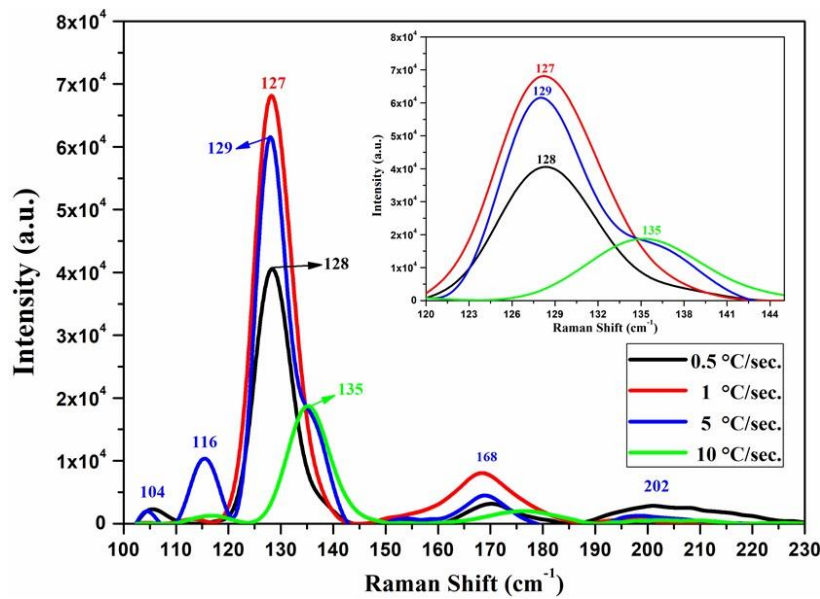

**Figure 2** Raman spectra of CIGT thin films reacted with different ramping rates

Table 2 . The peak positions observed and the reference values for the Raman modes

0.5°C/sec.	1°C/sec.	5°C/sec.	10°C/sec.	CIT (Ref.)	CGT (Ref.)
106	104	104	104	106[a] [B_2^2]	-
117	114	116	117	116[a] [B_1^2]	117[c],122[b] [A_2]
128	127	129	-	125[a] [A_1]	-
-	-	135	135	-	136[b], 138[c] [A_1]
-	168	168	-	162[a] [E_1^4]	-
170	-	-	177	170[a][E_1^5], [B_2^3]	173[b], 185[b] [B_2-E]
200	202	202	202	192[a][E_1^6]	205[b] [B_2 - E]

Ref.a [35, 36], Ref.b [37], Ref.c [38]

S. Erkan, Y. Atasoy, A. Çiriş, E. Bacaksız

3.3. Scanning Electron Microscope (SEM) Images

SEM images of CIGT samples reacted at different ramping rates are shown in Figure 3. It is clearly seen that the ramping rate has a significant effect on the surface morphology of the samples. When the surface image of the sample reacted at 0.5°C/sec was examined, the film surface was seen to have a porous structure. The grain formation started with the increase of the ramping rate and small-grained structure was formed instead of porous structure. In the sample reacting at 5°C/sec, it was formed in large grains with a size of 1-3 μm as well as small grains [39]. When the ramping rate increased to 10°C/sec, it was determined that the surface morphology completely changed, turning into a fused structure [40, 41].
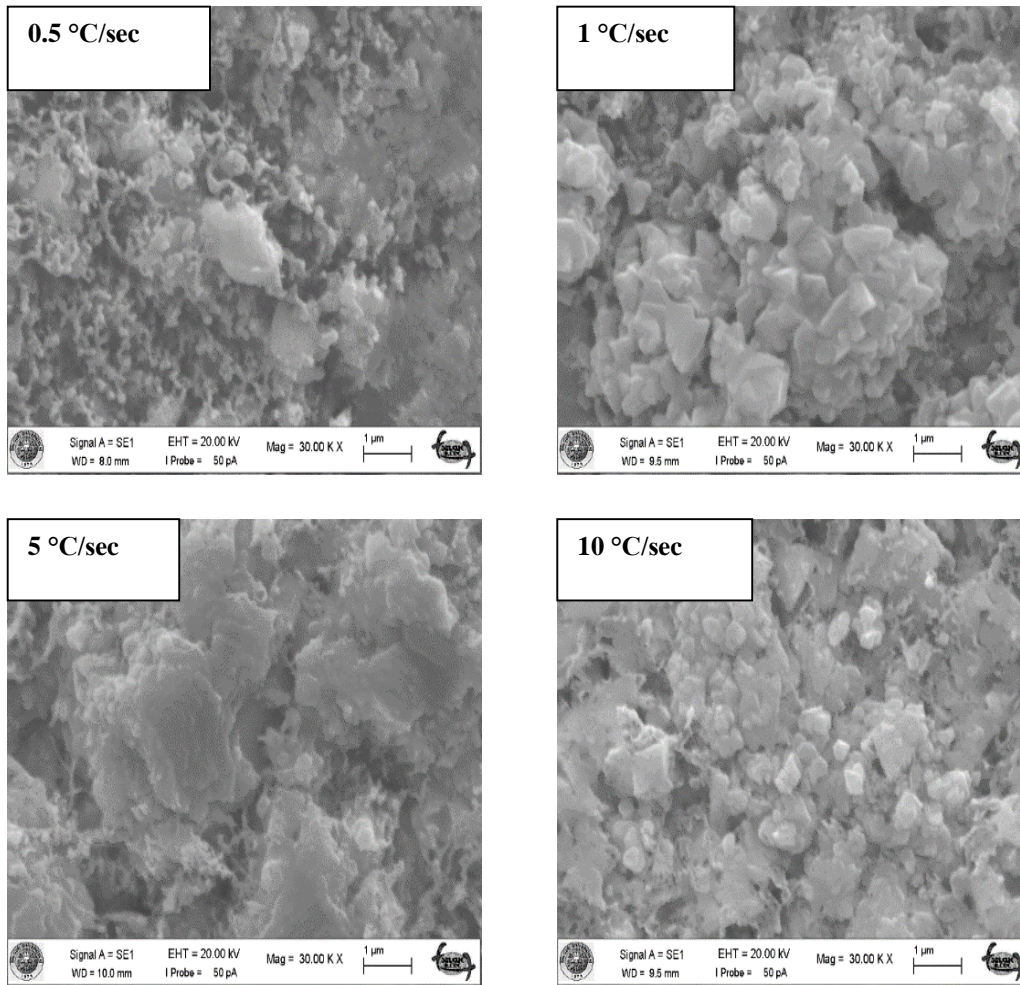
Figure 3 SEM images of CIGT samples reacted at different ramping rates

3.4. Energy Dispersive X-Ray Spectroscopy (EDS) Results

The atomic compositions and the ratios of metallic atoms of CIGT samples reacted at different ramping rates are shown in Table 3. The targeted metallic ratios in the samples are about 0.3 for [Ga]/([Ga]+[In]) and in the range of 0.7-0.9 for [Cu]/([In]+[Ga]). When the table examined, the samples were found to be consistent with the targeted metallic ratios, except for the sample reacting at 0.5°C/sec. In addition, all of the samples regardless of ramping rates were seen to be Te-poor.

INVESTIGATION OF THE EFFECT OF HEATING RAMP RATE ON CU(IN, GA)TE$_2$ THIN FILMS

Table 3 Atomic compositions and some metallic ratios of the CIGT samples

Elements	0.5 °C/sec	1 °C/sec	5 °C/sec	10 °C/sec
Atomic Compositions				
Cu (%)	17.65	29.91	24.44	22.99
In (%)	27.59	22.51	22.02	20.95
Ga (%)	8.96	13.88	11.10	11.61
Te (%)	45.81	33.69	42.66	44.45
Ratios of Metallic Atoms				
$\dfrac{(Cu)}{(In) + (Ga)}$	0.48	0.82	0.74	0.71
$\dfrac{(Ga)}{(In) + (Ga)}$	0.25	0.38	0.34	0.36

4. CONCLUSION

In this study, the effect of reaching the target annealing temperature at different ramping rates on the properties of CIGT thin films was investigated. CIGT thin films were produced by heat treating of foil/Mo/(Cu, In, Ga)/NaF/Te layered structure. In this layered structure, (Cu, In, Ga) precursors were grown by electro-deposition method and then NaF and Te layers were evaporated by electron beam. The annealing process of the samples was carried out with RTP furnace at the target temperature of 600°C for 5 minutes dwell time. To examine the effect of the ramping rate, the target annealing temperature was reached at the ramping rates of 0.5, 1, 5 and 10°C/sec.

XRD results showed that regardless of the ramping rate, all samples crystallized in the chalcopyrite CIGT structure and no secondary phases were formed. Considering the structural parameters such as FWHM and crystallite size of the samples, it was seen that crystal quality improved up to 5°C/sec ramping rate, but started to deteriorate at 10°C/sec. The Raman spectra demonstrated that the CIGT phase was formed at the ramping rates from 0.5 to 5°C/sec, but it was transformed into the CGT phase at 10°C/sec. SEM images showed that the porous structure turned into a large-small grain structure as a result of the increasing of ramping rate from 0.5 to 5°C/sec. However, it was observed that the surface morphology changed and fused structure was formed in the sample reacting at 10°C/sec. The EDS results revealed that the targeted ratios of metallic atoms were achieved, except for the 0.5°C/sec sample, however all samples were Te-poor.

When the characterization results of the samples are evaluated, it can be said that the CIGT absorber layer reacting at 5°C/sec is more suitable for photovoltaic applications.

REFERENCES

[1] Calixto, M., et al., *Compositional and optoelectronic properties of CIS and CIGS thin films formed by electrodeposition.* Solar energy materials and solar cells, 1999. 59(1-2): p. 75-84.

[2] Fernandez, A., et al., *Electrodeposited and selenized (CuInSe$_2$)(CIS) thin films for photovoltaic applications.* Solar Energy Materials and Solar Cells, 1998. 52(3-4): p. 423-431.

[3] Gordillo, G. and C. Calderon, *CIS thin film solar cells with evaporated InSe buffer layers.* Solar energy materials and solar cells, 2003. 77(2): p. 163-173.

[4]   Zaretskaya, E., et al., *Raman spectroscopy of CuInSe₂ thin films prepared by selenization.* Journal of Physics and Chemistry of Solids, 2003. 64(9-10): p. 1989-1993.

[5]   Caballero, R., et al. *CGS-thin films solar cells on transparent back contact.* in *2006 IEEE 4th World Conference on Photovoltaic Energy Conference.* 2006. IEEE.

[6]   Ishizuka, S., et al., *Structural tuning of wide-gap chalcopyrite CuGaSe₂ thin films and highly efficient solar cells: differences from narrow-gap Cu(In, Ga)Se₂.* Progress in Photovoltaics: Research and Applications, 2014. 22(7): p. 821-829.

[7]   Thirumalaisamy, L., et al., *Engineering of sub-band in CuGaS₂ thin films via Mo doping by chemical spray pyrolysis route.* Thin Solid Films, 2020. 709: p. 138252.

[8]   Aissaoui, O., et al., *Study of flash evaporated CuIn₁₋ₓGaₓTe₂ (x= 0, 0.5 and 1) thin films.* Thin Solid Films, 2009. 517(7): p. 2171-2174.

[9]   Jung, S., et al., *Effects of Ga contents on properties of CIGS thin films and solar cells fabricated by co-evaporation technique.* Current Applied Physics, 2010. 10(4): p. 990-996.

[10]   Li, W., et al., *Fabrication of Cu(In, Ga)Se₂ thin films solar cell by selenization process with Se vapor.* Solar Energy, 2006. 80(2): p. 191-195.

[11]   Zhou, D., et al., *Sputtered molybdenum thin films and the application in CIGS solar cells.* Applied Surface Science, 2016. 362: p. 202-209.

[12]   Green, M.A., et al., *Solar cell efficiency tables (Version 45).* Progress in photovoltaics: research and applications, 2015. 23(1): p. 1-9.

[13]   Kato, T., et al., *Record efficiency for thin-film polycrystalline solar cells up to 22.9% achieved by Cs-treated Cu(In, Ga)(Se, S)₂.* IEEE Journal of Photovoltaics, 2018. 9(1): p. 325-330.

[14]   Karatay, A., et al., *The effect of Se/Te ratio on transient absorption behavior and nonlinear absorption properties of CuIn₀.₇Ga₀.₃(Se₁₋ₓTeₓ)₂ (0≤x≤ 1) amorphous semiconductor thin films.* Optical Materials, 2017. 73: p. 20-24.

[15]   Gremenok, V., et al., *Characterization of polycrystalline Cu(In, Ga)Te₂ thin films prepared by pulsed laser deposition.* Thin Solid Films, 2001. 394(1-2): p. 23-28.

[16]   Başol, B.M., et al., *Cu(In, Ga)Se₂ thin films and solar cells prepared by selenization of metallic precursors.* Journal of Vacuum Science & Technology A: Vacuum, Surfaces, and Films, 1996. 14(4): p. 2251-2256.

[17]   Witte, W., R. Kniese, and M. Powalla, *Raman investigations of Cu(In, Ga)Se₂ thin films with various copper contents.* Thin Solid Films, 2008. 517(2): p. 867-869.

[18]   Witte, W., et al. *Influence of the Ga content on the Mo/Cu(In, Ga)Se₂ interface formation.* in *2006 IEEE 4th World Conference on Photovoltaic Energy Conference.* 2006. IEEE.

[19]   Rockett, A., et al., *Na in selenized Cu(In, Ga)Se₂ on Na-containing and Na-free glasses: distribution, grain structure, and device performances.* Thin Solid Films, 2000. 372(1-2): p. 212-217.

[20]   Sanad, M., M. Rashad, and A.Y. Shenouda, *Novel CuIn₁₋ₓGaₓTe₂ Structures for High Efficiency Photo-electrochemical Solar Cells.* Int. J. Electrochem. Sci, 2016. 11: p. 4337-4351.

[21]   Gaburici, D., et al., *Rapid Synthesis of Polycrystalline CuGa₁₋ₓInₓTe₂ Compounds.* Crystal Research and Technology: Journal of Experimental and Industrial Crystallography, 2000. 35(3): p. 265-270.

[22]   Rincón, C., S. Wasim, and G. Marín, *Effect of donor-acceptor defect pairs on the electrical and optical properties of CuIn₃Te₅.* Journal of Physics: Condensed Matter, 2002. 14(5): p. 997.

[23]   Rincón, C., et al., *Raman spectra of CuGa₃Te₅ ordered-defect compound.* physica status solidi (b), 2017. 254(9): p. 1600844.

[24]   Rincón, C., et al., *Raman spectra of CuInTe₂, CuIn₃Te₅, and CuIn₅Te₈ ternary compounds.* Journal of Applied Physics, 2000. 88(6): p. 3439-3444.

[25]   Rincón, C., et al., *Raman spectra of the chalcopyrite compound CuGaTe₂.* Journal of Physics and Chemistry of Solids, 2001. 62(5): p. 847-855.

[26]   Rincón, C., et al., *Raman spectra of the chalcopyrite compound CuGaTe₂.* Materials Letters, 1999. 38(4): p. 305-307.

[27]   Wasim, S., et al., *On the band gap anomaly in I–III–VI₂, I–III₃–VI₅, and I–III₅–VI₈ families of Cu ternaries.* Applied Physics Letters, 2000. 77(1): p. 94-96.

[28]   Salem, A., et al., *Synthesis and Electrical Transport Properties of CuInGaTe₂.* J Laser Opt Photonics, 2018. 5(183): p. 2.

[29] Chandramohan, M., S. Velumani, and T. Venkatachalam, *Experimental and theoretical investigations of structural and optical properties of CIGS thin films.* Materials Science and Engineering: B, 2010. 174(1-3): p. 205-208.

[30] Badgujar, A.C., S.R. Dhage, and S.V. Joshi, *Process parameter impact on properties of sputtered large-area Mo bilayers for CIGS thin film solar cell applications.* Thin Solid Films, 2015. 589: p. 79-84.

[31] Hsu, W.-H., et al., *Controlling morphology and crystallite size of Cu(In$_{0.7}$Ga$_{0.3}$)Se$_2$ nano-crystals synthesized using a heating-up method.* Journal of Solid State Chemistry, 2013. 208: p. 1-8.

[32] Atasoy, Y., et al., *Cu(In, Ga)(Se, Te)$_2$ films formed on metal foil substrates by a two-stage process employing electrodeposition and evaporation.* Thin Solid Films, 2018. 649: p. 30-37.

[33] Ananthan, M., B.C. Mohanty, and S. Kasiviswanathan, *Micro-Raman spectroscopy studies of bulk and thin films of CuInTe$_2$.* Semiconductor science and technology, 2009. 24(7): p. 075019.

[34] Ntholeng, N., *Synthesis and characterization of Cu-based telluride semiconductor materials for application in photovoltaic cells.* 2017.

[35] Roy, S., et al., *CuInTe$_2$ thin films synthesized by graphite box annealing of In/Cu/Te stacked elemental layers.* Vacuum, 2002. 65(1): p. 27-37.

[36] Roy, S., et al., *Synthesis of CuInTe$_2$ by rapid thermal annealing of In/Cu/Te stacked elemental layers.* physica status solidi (a), 2002. 189(1): p. 209-221.

[37] Aksu, S., J. Wang, and B.M. Basol, *Electrodeposition of In–Se and Ga–Se thin films for preparation of CIGS solar cells.* Electrochemical and Solid-State Letters, 2009. 12(5): p. D33-D35.

[38] Wasim, S., et al., *Effect of donor–acceptor defect pairs on the crystal structure of In and Ga rich ternary compounds of Cu–In(Ga)–Se(Te) systems.* Journal of Physics and Chemistry of Solids, 2005. 66(11): p. 1990-1993.

[39] Venkatachalam, M., et al., *Investigations on electron beam evaporated Cu(In$_{0.85}$Ga$_{0.15}$)Se$_2$ thin film solar cells.* Solar Energy, 2009. 83(9): p. 1652-1655.

[40] Fiat, S., et al., *The influence of stoichiometry and annealing temperature on the properties of CuIn$_{0.7}$Ga$_{0.3}$Se$_2$ and CuIn$_{0.7}$Ga$_{0.3}$Te$_2$ thin films.* Thin Solid Films, 2013. 545: p. 64-70.

[41] Strzhemechny, Y., et al., *Near-surface electronic defects and morphology of CuIn$_{1-x}$Ga$_x$Se$_2$.* Journal of Vacuum Science & Technology B: Microelectronics and Nanometer Structures Processing, Measurement, and Phenomena, 2002. 20(6): p. 2441-2448.